Ureña, N. Multiblock copolymers of sulfonated PSU/PPSU Poly(ether sulfone)s as solid electrolytes for proton exchange membrane fuel cells, In *Electrochimica Acta, 302, April 2019, Pp. 428-440*

DOI: https://doi.org/10.1016/j.electacta.2019.01.112

Accepted Manuscript

Multiblock copolymers of sulfonated PSU/PPSU Poly(ether sulfone)s as solid electrolytes for proton exchange membrane fuel cells

Nieves Ureña, María Teresa Pérez-Prior, Carmen del Río, Alejandro Várez, Jean-Yves Sanchez, Cristina Iojoiu, Belén Levenfeld

PII: S0013-4686(19)30131-8

DOI: https://doi.org/10.1016/j.electacta.2019.01.112

Reference: EA 33515

To appear in: *Electrochimica Acta*

Received Date: 20 November 2018

Revised Date: 30 December 2018

Accepted Date: 20 January 2019

Please cite this article as: N. Ureña, Marí.Teresa. Pérez-Prior, C.d. Río, A. Várez, J.-Y. Sanchez, C. Iojoiu, Belé. Levenfeld, Multiblock copolymers of sulfonated PSU/PPSU Poly(ether sulfone)s as solid electrolytes for proton exchange membrane fuel cells, *Electrochimica Acta* (2019), doi: https://doi.org/10.1016/j.electacta.2019.01.112.

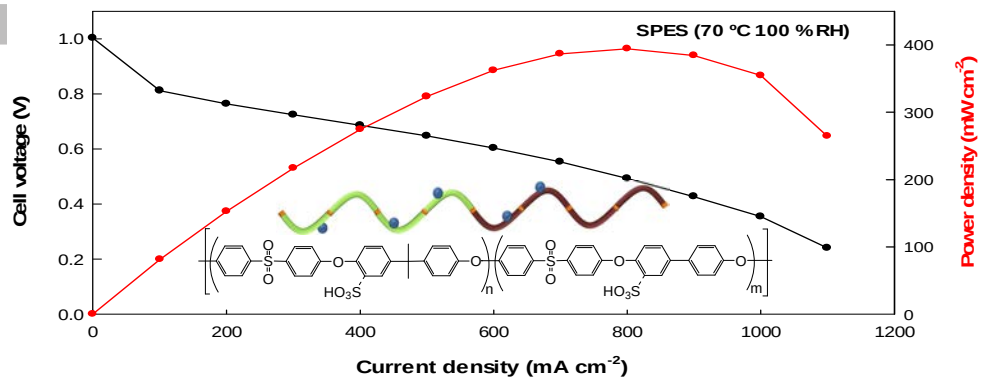

Multiblock Copolymers of Sulfonated PSU/PPSU Poly(ether sulfone)s as Solid Electrolytes for Proton Exchange Membrane Fuel Cells

Nieves Ureña [a], María Teresa Pérez-Prior [a], Carmen del Río [b], Alejandro Várez [a], Jean-Yves Sanchez [a,c,d], Cristina Iojoiu [c,d], Belén Levenfeld [a]

[a]Universidad Carlos III de Madrid. Departamento de Ciencia e Ingeniería de Materiales e Ingeniería Química, IAAB. Avda. Universidad, 30, 28911 Leganés, Madrid, Spain.

[b]Instituto de Ciencia y Tecnología de Polímeros (ICTP-CSIC). C/Juan de la Cierva, 3, 28006 Madrid, Spain.

[c]Univ. Grenoble Alpes, LEPMI, 38000 Grenoble, France.

[d]CNRS, LEPMI, 38000 Grenoble, France.

*Corresponding author. Tel.: +34 91 624 83 74

E-mail address: mailto:maperezp@ing.uc3m.es

Abstract

Sulfonated multiblock copolymers composed of Polysulfone (PSU) and Polyphenylsulfone (PPSU) poly(ether sulfone) segments (SPSU/SPPSU) are synthesized for the first time by polycondensation in a "one-pot two-step synthesis" of commercial monomers, followed by sulfonation reaction with trimethylsilyl chlorosulfonate (TMSCS). Both segments are responsible for proton conductivity, although the PSU block has greater affinity to be sulfonated. Even though no microphase separation is detected, the resulting ionomers exhibit good mechanical properties due to the non-sulfonated blocks remaining and to the high molecular weights of the ionomers. The chemical structure is confirmed by ^{1}H-NMR, ^{19}F-NMR and FTIR analysis. The degree of sulfonation (0.93-1.58) is determined from the IEC values and ^{1}H-NMR spectra. In situ through-plane proton conductivity measured on the MEAs is 34.1 mS cm^{-1} at 70 ˚C. A maximum power density of 400 mW cm^{-2}, a current density of 1100 mA cm^{-2} and outstanding thermo-mechanical stability, these proton-conducting membranes can therefore be implemented in PEMFC.

Keywords: Block copolymer; sulfonation; polysulfone; PEMFC; proton exchange membranes.

Abbreviations

FCs Fuel cells
PEMFCs Proton exchange membrane fuel cells
PEM Proton exchange membrane
PFSA Perfluorosulfonic acid
PBI Polybenzimidazole
SPEEK Sulfonated poly(ether ether ketone)
T_m Melting temperature
PES Poly(ether sulfone)
PSU Polysulfone
DS Degree of sulfonation
WU% Water uptake
TS Tensile strength
PPSU Polyphenylsulfone
PSU/PPSU PES copolymers of PSU and PPSU segments
^{1}H-NMR Proton nuclear magnetic resonance spectroscopy
FTIR Infrared spectroscopy
SEC Size exclusion chromatography
SEC-MALLS Size exclusion chromatography multi-angle laser light scattering
MEA Membrane electrode assembly
DMSO Dimethyl sulfoxide
DMAc *N*,*N*-dimethylacetamide
DGME Diethyleneglycol-monomethyl-ether
TMSCS Trimethylsilyl chlorosulfonate
DCE 1,2-Dichloroethane
DMF Dimethylformamide
DFDPS 4,4'-Difluoro-diphenylsulfone
BPA 4,4'-Isopropylidenediphenol
BP 4,4'-Dihydroxybiphenyl
DHDPS 4,4'-Dihydroxydiphenylsulfone

SPES Sulfonated PES copolymers of PSU and PPSU segments

IEC Ion-exchange capacity

TGA Thermogravimetric analysis

T_{OD} Onset decomposition temperature

T_{FD} Fastest decomposition temperature

DSC Differential scanning calorimetry

FEG-SEM Field emission gun scanning electron microscopy

BSE Energy selective backscatter

DMA Dynamo mechanical analysis

EIS Electrochemical impedance spectroscopy

σ_m Membrane ionic conductivity

MWD Molecular weight distribution

I_p Polydispersity index

M_n Number average molecular weight

MHS Mark-Houwink-Sakurada

LS Light scattering

M_w Weight average molecular weight

T_g Glass transition temperature

AN Acceptor number

T_α Temperature associated with a α relaxation

1. Introduction

The greenhouse effect has received more attention in recent years due to large amount of harmful gas emissions, such as CO_2, that are released to the atmosphere. Thus, in 2015, global CO_2 emissions from fuel combustion reached 32.3 $GtCO_2$ [1]. To reduce the human contribution of CO_2 emissions, it is mandatory to efficiently store carbon-free or low-carbon renewable electricity. Less crucial for emissions, but necessary to decrease urban pollution, is electromobility, which is now attracting increased interest. Electrochemical energy storage (batteries, supercapacitors) and conversion (Fuel Cells, FCs) are currently the best solutions to cut both urban pollution and CO_2 emissions. Proton exchange membrane fuel cells (PEMFCs) have been proposed as promising energy sources in diverse applications such as transportation, stationary energy, and even portable devices [2,3]. In PEMFCs, one of the critical components remaining is the proton exchange membrane (PEM). To date, perflurosulfonic acid ionomers (PFSA), e.g., Nafion® (long side-chains) or Aquivion® (short side-chains) are still considered a reference electrolyte of PEMFC but also an unavoidable binder of electrodes [4]. Due to its superacid groups, the outstanding commercial Nafion membrane provides high conductivities and high oxidative stability, leading to high performance and durability in PEMFCs [5,6]. However, Nafion displays disadvantages such as poor thermo-mechanical stability, high oxygen permeability [7], and high cost. In addition, this membrane undergoes degradation in real devices [8,9]. These drawbacks necessitate the search for other ionomers based on different polymeric backbones [10]. A comparison of the advantages and drawbacks of possible ionomer backbones is presented by Iojoiu et al. [11].

PEMs synthesized from poly(benzimidazole) (PBI) show high mechanical and thermal stability [12,13], but their blends with phosphoric acid are above all considered for high-temperature PEMFC implementation. Sulfonated aromatic main-chain polymers have received attention due to their excellent properties, such as low cost and high chemical and thermal stabilities [10]. In particular, sulfonated poly(ether ether ketone) (SPEEK) have been extensively used [14,15] in polymer blends [16,17], copolymers [18], and as part of composites [19]. PEEK, due to its high crystallinity and melting temperature (T_m), is considered one of the best thermoplastics, but its sulfonation, typically achieved in highly concentrated sulfuric acid, makes its purification fairly difficult. Moreover, its main assets, i.e., high crystallinity and T_m, vanish in highly conducting sulfonated ionomers. Membranes based on amorphous poly(ether sulfone) (PES) have also been considered potentially viable for fuel cell applications [20,21]. Specifically, the use of polysulfone (PSU) as a backbone in the synthesis of PEMs, has been evident in the large number of research articles published in recent years [22-27].

Aryl-sulfonic based ionomers can be obtained either by a polycondensation involving an acidic monomer or by sulfonating a polymer bearing aryl-based repeat units. The bottom-up approach from ionic monomer to ionomers allows predicting and perfectly controlling the degree of sulfonation (DS). Nonetheless, the obtaining of a polycondensation grade i.e., a purity allowing a stoichiometric balance between the ionic and the other monomers is far from being easy, especially at the industrial scale. In contrast, the ionomer synthesis by post-sulfonation of polycondensates is well-mastered and easier; hence paving the way to lower production costs [28,29].

Membrane properties depend not only on the DS of the polymer but also on the experimental conditions used in the sulfonation reaction [26,30]. The proton

conductivity of PEMs can be generally favoured when the percentage of sulfonic groups increases [27], but this fact is accompanied by high water uptake (WU%), leading to the loss of dimensional stability of the membranes and their water dissolution.

Multiblock copolymers have recently attracted attention as starting materials for membrane synthesis due to their robust chemical structure, which is characterized by good mechanical properties, even when there are many functional groups [31]. Sannigrahi and coworkers [32] have prepared block copolymers based on the combination of both hydrophilic sulfonated polysulfone and hydrophobic aromatic polyfluoroether segments. As a result, mechanically robust membranes with a very high proton conductivity of 100 mS cm^{-1} under fully hydrated conditions and 80 ˚C are obtained. Membranes based on sulfonated PEEK-b-PES copolymers also exhibit high conductivities of approximately 200 mS cm^{-1} and excellent dimensional stability, i.e., the tensile strength (TS), and the elongation at break of the membranes are in the range of 23-35 MPa and 20-51% [33]. In this case, sulfonation occurred on the anisole groups and not the polymeric backbone, allowing PEEK crystallinity to be suppressed. In addition, copolymers based on sulfonated and non-sulfonated PSU or fluorinated PES polymers are synthesized using an ionic monomer (sulfonated diphenol) and are successfully used as membranes for FC applications [20,21]. Thus, a powerful copolymer structure in multiblocks, which can be used to prepare PEMs, has been proposed as a main goal in this research field. Among high-performance polymer backbones, amorphous PES are likely the best candidates, since they (i) do not face the sulfonation issues of PEEK related to their high crystallinity, (ii) are not sensitive to hydrolysis as polyimides and (iii) have a low brittle-ductile transition related to their low transition, T_β, which is close to -123 ˚C. For these reasons, we based our polycondensated multiblock on PES alternating PSU and polyphenylsulfone (PPSU)

blocks (PSU/PPSU). In our case, sulfonated multiblock ionomers are obtained via an easy process composed of a "one-pot two-step synthesis" followed by their sulfonation. This approach has several advantages, namely: (i) it reduces the number of synthesis steps compared with the usual polycondensation, which comprises three steps (two steps for the synthesis and purification of the two oligomers and one step for their copolycondensation), (ii) it allows obtaining high molecular weight using commercial monomers of high purity, and (iii) sulfonation of high performance polymers is well-mastered. Additionally, this approach allows decreasing the solvent volumes used and the overall reaction time. The present work also includes molecular characterization of the copolymers by proton nuclear magnetic resonance spectroscopy (^{1}H-NMR), infrared spectroscopy (FTIR), size exclusion chromatography and size exclusion chromatography multi-angle laser scattering (SEC and SEC-MALLS). The morphology of the polymeric membranes is evaluated through scanning electron microscopy. The properties of thermal stability, WU%, dynamo mechanical behaviour, and membrane ionic conductivity are also investigated and compared with other sulfonated polymers. Furthermore, the membrane electrode assembly (MEA) performance of this material is also tested.

2. Experimental procedure

2.1 Materials and reagents

Dimethyl sulfoxide-d_6 (DMSO-d_6, 99.9%), *N*,*N*-dimethylacetamide (DMAc, 99.0%), potassium carbonate (K_2CO_3, ≥ 99.0%), and diethyleneglycol-monomethyl-ether (DGME, 98%) were purchased from Acros Organics and used as received. Chloroform-d ($CDCl_3$-d, 99.9% D), trimethylsilyl chlorosulfonate (TMSCS, 99.0%), 1,2-dichloroethane (DCE, 98.9%), dimethylformamide (DMF, ≥ 99.8%), and toluene

(99.8%) were supplied by Sigma-Aldrich. The 4,4'-difluoro-diphenylsulfone (DFDPS), 4,4'-isopropylidenediphenol (BPA), 4,4'-dihydroxybiphenyl (BP), 4,4'-dihydroxydiphenylsulfone (DHDPS), were purchased from Alfa Aesar and recrystallized from isopropanol before use.

2.2 Synthesis of copolymer backbone

2.2.1 Synthesis of PSU/PPSU copolymer

As shown in Scheme 1, the multiblock copolymer was synthesized via polycondensation in a "one-pot two-step synthesis". The synthesis pathway was performed as follows. First, 4.00 g (15.73 mmol) of DFDPS, 3.18 g (17.09 mmol) of BP, and 7.08 g (51.29 mmol) of anhydrous K_2CO_3 were added to a three-neck round-bottom flask provided with mechanical stirring, argon inlet and a dean-stark trap. The reagents, DFDPS and BP, were dissolved in DMAc (29 mL). Toluene (15 mL) was added as an azeotropic agent for water removal. The reaction mixture was heated at reflux to 160 ˚C and kept at this temperature for 4 h to dehydrate the system. The temperature was increased to 180 ˚C to eliminate the toluene. After distillation, the solution was maintained at 120 ˚C for 18 h. Once the reaction was over, 2.91 g (12.74 mmol) of BPA dissolved in 7 mL of DMAc, 5.28 g (38.24 mmol) of K_2CO_3, and 13 mL of toluene were added. The azeotropic process was performed a second time. Just before distilling off the toluene, 3.58 g (14.11 mmol) of DFDPS dissolved in 19 mL of DMAc were injected into the flask. The mixture reacted for 18 h and acquired a high viscosity. The copolymer was isolated by precipitation in a 1 M HCl solution. Finally, the resulting precipitate was dried under vacuum at 60 ˚C for 48 h.

2.2.2 Sulfonation of PSU/PPSU copolymer

The sulfonation of PSU/PPSU copolymer was performed according to the procedure described by Chao et al. [34] with minor modification. The reaction was performed under anhydrous conditions in a three-neck round-bottom flask equipped with an argon inlet, magnetic stirring and a dean-stark trap. As shown in Scheme 2, 5.00 g of copolymer was dissolved in 50 mL of DCE at room temperature. Once PSU/PPSU was totally dissolved, the temperature was increased to 90 ˚C to remove the water by azeotropic distillation (approximately 20 mL). When water from the copolymer solution was removed, the temperature of the mixture was decreased at R.T., and TMSCS, which was used as sulfonating agent, was diluted in dried DCE and added dropwise to the flask. To obtain varying degrees of sulfonation, volumes of TMSCS which ranged from 5.23 mL to 20.89 mL were employed. The reaction was maintained for 24 h. The obtained sulfonated copolymer was precipitated in a 0.1 M NaOH solution and then filtered and washed with deionized water to neutral pH and dried under vacuum at 60 ˚C for 24 h.

In this work, the initial copolymer PSU/PPSU is abbreviated as PES in the results and discussion section. The synthesized SPSU/SPPSU membranes are abbreviated as SPES. The number of samples of SPES are denoted as a function of the amount of sulfonating agent added in the sulfonation reaction of the copolymers. Table 1 shows the PSU unit: TMSCS molar ratios used in the synthesis.

Table 1. PSU unit: TMSCS molar ratios used in sulfonation reaction for prepared membranes

Membrane	PSU unit: TMSCS
SPES 1	1:3
SPES 2	1:6
SPES 3	1:9

2.2.3 Membrane preparation

The SPES copolymer was dissolved (5 wt %) in DMF, and the resulting solution was cast onto a petri glass and dried under vacuum using a ramp of temperature, which ranged between 30 and 80 ˚C over 48 h. The thickness of the obtained membranes was 50-75 µm. Afterwards, the SPES membrane in the Na^+ salt form was immersed in a 1 M HCl solution at 60 ˚C during 24 h to replace Na^+ with H^+ to obtain membrane in the acidic form.

2.3 Measurements

2.3.1 ^{1}H-NMR and ^{19}F-NMR

All copolymers were analysed by ^{1}H-NMR spectroscopy, employing a Bruker WM 250 spectrometer at 300.12 MHz. In the case of ^{19}F-NMR, the frequency was 282.39 MHz. The initial copolymer PSU/PPSU was dissolved in $CDCl_3$ and the sulfonated copolymers in DMSO-d_6. Tetramethylsilane was used as the internal reference.

2.3.2 Acid-base titration

2.3.2.1 Ion-exchange Capacity (IEC) by standard method

The IEC of the SPES membranes was determined by acid-base titration. First, dry membranes in the Na^+ form were immersed in a 1 M HCl aqueous solution for 24 h at 60 ˚C to obtain the acidic form, and then in a 2 M NaCl aqueous solution for 24 h to replace H^+ with Na^+. The resulting solutions were titrated using a 0.01 M NaOH aqueous solution, which was previously normalized with a solution of potassium

hydrogen phthalate. Phenolphthalein was used as an indicator. The titrations were repeated three times per sample. The IEC values were calculated as follows [35]:

$$IEC = \frac{V_{NaOH} \times [NaOH]}{W_{dry}} \quad (1)$$

where V_{NaOH} and [NaOH] are the volume and concentration of NaOH used in the titration, respectively, and w_{dry} is the weight of the dry membranes.

2.3.2.2 IEC by titration in organic medium

The IEC was also determined by titration in the presence of DGME as the organic solvent and methyl orange as the indicator. The dry membranes in the Na^+ form were immersed in a 1 M HCl solution for 24 h at 60 ˚C. Then, the membranes were washed with deionized water and dried under vacuum during 24 h to remove the water. The resulting membranes were dissolved in DGME. Once dissolved, the solutions were titrated using a 0.05 M NaOH solution in triplicate. IEC values were calculated using Eq. (1) as previously shown.

2.3.3 FTIR

The FTIR spectra of the membranes were recorded in a Perkin-Elmer Spectrum GX Instrument in the range of 4000-400 cm^{-1} at a resolution of 4 cm^{-1} and 16 scans. Spectra are shown in the supporting information (Figure 2S).

2.3.4 SEC and SEC-MALLS

SEC and SEC-MALLS analyses were performed in a SOPARES RI2000 differential refractometer coupled to a WYATT DAWN EOS light scattering detector with a 2xPLgel-Mixed-D column. The pump was a Waters 515 HPLC. Measurements were performed at 70 ˚C at a flow rate of 1 mL min^{-1}. A solution of 0.1 M $NaNO_3$ in DMF was used as a solvent. The sample solutions were previously filtered with a 0.45-

µm Millipore or PTFE filter. The molecular weights of the copolymers were referenced to polystyrene standards.

2.3.5 Thermogravimetric analysis (TGA)

A Pyris TGA1 instrument from Perkin-Elmer was employed to assess the thermal stability of the PEMs. The membrane sample (10.0 mg) was heated from 40 to 600 ˚C at a rate of 10 ˚C min^{-1} under air. The thermal behaviour of the sulfonic groups was evaluated using the temperature from which the weight loss begins (onset decomposition temperature, T_{OD}) and the temperature of the maximum in the weight loss rate (fastest decomposition temperature, T_{FD}). The temperature at which a 5% weight loss occurred was chosen as the reference degradation temperature of the samples and was denoted as $T_{d5\%}$. Isotherms (weight loss *versus* time) were performed at 100 ˚C for 12 h under air flow to study the thermal durability of the membranes.

2.3.6 Differential Scanning Calorimetry (DSC)

DSC analysis was performed on a membrane sample (7.5-10.0 mg) from 50 to 350 ˚C at a heating rate of 10 ˚C min^{-1} under N_2. A Mettler Toledo 822 instrument was used for the DSC measurements.

2.3.7 Field Emission Gun Scanning Electron Microscopy (FEG-SEM)

The morphology of membranes was characterized by FEG-SEM using a ZEISS Ultra 55 equipped with a backscattered electron detector that enables energy selective backscatter (BSE) imaging. FEG-SEM images were recorded operating at 3 kV. For a better inspection in FEG-SEM of a possible phase separation, mobile H^+ coming from sulfonic groups were replaced by Pb^{2+} ions. First, the membranes in the Na^+ form were immersed in a 1 M HCl solution several times to replace Na^+ with H^+. The resulting membranes were repeatedly rinsed with deionized water. Finally, the membrane

samples were immersed in a 1 M $Pb(NO_3)_2$ solution stirred for 48 h and dried in an oven at 60 ˚C. A representative image is shown in the supporting information (Figure 3S).

2.3.8 WU%

The parameter of WU% were evaluated in the range of temperature from R.T. to 60 ˚C. The thickness of the membranes was approximately 75 µm. First, the samples were dried under vacuum at 60 ˚C to obtain the weight of the dry membranes, w_{dry}. Then, the samples were immersed in deionized water for 72 h. Before obtaining the weight of the wet membranes, w_{wet}, the excess surface water was removed with blotting paper. This process was systematically and quickly repeated three times at each temperature and for each sample. Thus, WU% was calculated according to Eq. (2) [36].

$$WU\% = \frac{W_{wet} - W_{dry}}{W_{dry}} \times 100 \quad (2)$$

2.3.9 Mechanical properties

The Dynamo Mechanical analysis (DMA) in the tensile mode was performed using DMA Q800 equipment (TA Instruments, USA). The width and length of the analysed samples were 2.5 and 12.0 mm, respectively, and the thickness was approximately 50 µm. An initial static force of 0.15 N was employed in all experiments. Stress-Strain test conditions were fixed at 30 ˚C in controlled force mode at a ramp force of 0.3 N min^{-1}, reaching 18.0 N. The frequency used was 1 Hz and the measurements were performed by heating from 30 to 250 ˚C with a rate of 2 ˚C min^{-1}. Experiments were performed using membranes in the Na^+ form that were previously dried under vacuum for 48 h at 100 ˚C to remove embedded water. Another set of experiments were performed on wet membranes which were tested directly after being immersed in a 1 M HCl solution for 24 h at 60 ˚C to obtain the H^+ form. Each test was repeated at least three times, and the average value was considered.

2.3.10 Proton Conductivity

Proton conductivity measurements were determined via Electrochemical Impedance Spectroscopy (EIS) using a Material Mates 7260 frequency response analyser. The measurements were conducted in a frequency range between 10^{-1} and 10^{6} Hz using a voltage amplitude of 0.01 V. The influence that both temperature and relative humidity have on the electrochemical behaviour of the membranes was evaluated by varying (i) the temperature from 20 to 80 ˚C at a RH of 95%, and (ii) RH from 30 to 95% at a temperature of 80 ˚C. Both parameters, temperature and RH, were controlled in a Vösch 4018 climatic chamber. The test cell was composed of two gold electrodes separated by the membrane. The intercept point with the real axis in the Nyquist plot at high frequencies was considered to determine the resistance values. The proton conductivity of the membrane (σ_m) was determined from the resistance value via Eq. (3).

$$\sigma_m = \frac{L}{R_m \times A} \quad (3)$$

where L, R_m, and A are the thickness, resistance, and active area of the membrane.

The experimental data resulting from the EIS measurements were analysed using Z-View analysis impedance software (Scribner Associates, Inc., Southern Pines, NC, USA).

2.3.11 MEA test

Performance tests of MEA were performed in a Scribner 850e multi-range fuel cell test system. Pure hydrogen and pure oxygen were used as fuel and oxidant, respectively, at a flow rate of 200 mL min^{-1}. The measurements were performed at atmospheric pressure, 100% of relative humidity, and temperature from 50 to 80 ˚C. The membrane thickness was in the range of 50-60 µm. Cathode and anode catalyst

layers consisted of Pt/C catalyst (70 wt % Pt, Paxitech) (0.5 mg Pt cm^{-2}). The polarization curves were recorded after the single cell had reached stable conditions, i.e., the potential remained constant over time at a fixed current.

The in situ through-plane proton conductivity of the membranes was conducted using Electrochemical Impedance Spectroscopy on the MEA at 100% relative humidity and different cell temperatures using a potentiostat Autolab PGStat30 provided with an FRA module. During testing, the system was supplied with humidified hydrogen (SHE, anode) and nitrogen (cathode) at a flow rate of 200 mL min^{-1}. The amplitude sinusoidal signal was 10 mV, and the frequency was in the range between 100 kHz and 10 Hz. A DC bias potential of 0.45 V was used to record the spectra. The conductivity values were calculated according to Eq. (3). Each sample was measured at least five times after it reached a constant value to ensure good data reproducibility.

3. Results and Discussion

3.1.1. Strategy

Obtaining proton exchange membranes that can operate in a wide temperature range (i.e., from sub-ambient temperatures to at least 90 ˚C) requires finding a balance between two opposing membrane characteristics: high conductivity that requires a high concentration in hydrophilic aryl sulfonic acids but a moderate WU% to avoid excessive swelling of the membranes. To avoid extensive swelling of sulfonated membranes in FCs, two main approaches have been considered: (i) the filling of sulfonated ionomers (composite membranes) by proton-conducting inorganic materials [37,22] endowed with high conductivity and (ii) the synthesis of multiblock copolymers with alternating hydrophobic and hydrophilic blocks [38]. The Holy Grail is to prepare proton-

conducting blocks using ionic monomers, but these are not commercially available. Furthermore, their required purity grade faces upscaling issues that increase ionomer and membrane costs. For this reason, we decided to first prepare a polycondensated multiblock copolymer based on high-purity, commercial, cheap monomers that are used in the production of commercial PES and whose trademarks are Udel® and Radel®, and then to functionalize them exclusively or, if not possible, to preferentially functionalize one of them. The best route to obtain polycondensated multiblock copolymers consists of preparing and isolating linear blocks (i.e., cycle-free) obtained via monitored stoichiometric imbalance (i) to obtain the suited chain length, and (ii) to end-cap the resulting oligomers with suitable functions, allowing further polycondensation. These oligomers are reacted in a 1:1 stoichiometric ratio to obtain the targeted polyconsensated multiblock. While this is perfectly feasible in high yield at the lab-scale, this synthesis protocol is costly, and its upscaling is therefore questionable. We therefore opted for a "one-pot two-step synthesis", which is less ideal than the method described above but is likely to allow further upscaling.

3.1.2. Synthesis and characterization of SPES copolymers

3.1.2.1. Synthesis and spectroscopic characterizations

The synthesis of PSU/PPSU multiblock copolymers is performed by polycondensation in a "one-pot two-step synthesis" (Scheme 1). To obtain a 50:50 ratio of both blocks in the copolymer, the molecular weight of both segments is fixed at 5000 g mol^{-1} by controlling the molar ratio between the monomers BPA:DFDPS and BP:DFDPS. In a first step, a 5000 g mol^{-1} PPSU block end-capped by phenates is synthesized by reacting DFDPS and BP, using a stoichiometric imbalance, i.e., a slight excess (~ 11%) of BP. The reaction is monitored by ^{19}F-NMR, i.e., by the disappearance of fluorine signal from DFDPS. In the second step, the 5000 g mol^{-1} PSU

block is synthesized by adding BPA and DFDPS to a solution of the PPSU block. The successful formation of the PES multiblocks is confirmed by ^{1}H-NMR analysis (Figure 1). The characteristic peaks of both blocks in the range of δ between 6.80 and 8.00 ppm (H_1, H_2, H_3, and H_4 in the PSU block and H_5, H_6, H_7, and H_8 in the PPSU block) are verified by ^{1}H-NMR spectroscopy [30]. The number structural units of PPSU and PSU blocks are m = 12.5 and n = 11.3, respectively. The PSU/PPSU molar ratio roughly corresponds to the expected value, i.e., m/n = 1.1.

Except for PEEK, which requires sulfuric acid as both the solvent and reactant [14,39], the most common sulfonation reagent is $ClSO_3H$. This superacid is highly reactive but has two main drawbacks. First, if sulfonation occurs in a halogenated solvent, a precipitate forms as the ionomer is in its acidic form (hydrophilic), while the solvent is hydrophobic. This precipitation likely leads to heterogeneous reactions between the precipitate and reactant. Then, $ClSO_3H$ drastically decreases the intrinsic viscosity of sulfonated PES [23]. Due to the hydrophobic nature of the trimethylsilyl ester, sulfonation by the milder reagent TMSCS can be performed without precipitation. After electrophilic substitution, the ionomer can be indifferently precipitated, either in its sulfonic form (H^+) or its sulfonate form (Na^+ or Li^+). The precipitation of the acidic form is not easy [40]. If the sulfonation is performed under sufficient flux of inert gas (N_2 or Ar), no chain breakage is observed [30]. The BPA of the PSU block has two electron-donating groups: the ether group (-I, +M) and the isopropylidene group (+I). The latter decreases from ortho to meta but remains as a donating group, while the donating resonance effect of the ether outweighs its electron-withdrawing effect in the ortho position. Thus, both groups orient electrophilic substitution to the ortho position of BPA, while the ether is the sole electron-donating group in BP. To prove this fact, the

DS of both blocks are calculated through ^{1}H-NMR analysis and IEC as determined by chemical titrations.

The peak associated with the protons adjacent to the attached sulfonic groups is clearly upshifted. In the PSU segment, it shifts from 7.25 to 7.69 ppm (4''), while in the case of the PPSU unit, it shifts from 7.60 to 8.06 ppm (5''). Unfortunately, in the 7.60-7.80 ppm range, the peak denoted as 4'' is overlapped by peaks 5 and 5' in the PPSU block. Thus, ^{1}H-NMR spectra do not allow accurate determination of the degree of sulfonation of PSU blocks. However, the peak at δ = 8.06 ppm (5'') associated with the PPSU repeat unit is well defined (Figure 2), appearing in the two spectra (SPES 1 and 2), and its intensity increases significantly with the amount of sulfonating agent.

For this reason, the DS of the PPSU repeat unit is calculated according to Eq. (4) using the integral area of the peaks at 8.06 ppm (A(5'')), and 1.70 ppm (A(9)), which are associated with the 5'' peak of the PPSU block and isopropylidene moiety (9) (as shown in Figure 1S of the supporting information) of the PSU block, respectively.

$$DS_{NMRPPSU} = \frac{6A(5'')}{(A(9)\times 1.1)} \quad (4)$$

The DS of the PSU segment is also estimated from IEC values by subtracting the DS from PPSU units. The IEC is measured both by heterogeneous standard titration and by homogeneous titration of SPES organic solutions (Table 2). The IEC values determined using both methods are not significantly different, and a similar tendency is observed when the percentage of sulfonic groups increases in the copolymer. Thus, IEC varies from 1.01 (SPES 1) to 1.58 meq H^{+} g^{-1} (SPES 3) using standard heterogeneous titration and from 0.94 to 1.65 meq H^{+} g^{-1} using homogeneous titration of the ionomer solution. These results are analogous to the reported values of IEC for copolymers based on sulfonated PEEK-b-PES [33].

An estimation of the DS for the PSU unit (DS_{PSU}), is obtained using Eq. (5).

$$DS_{PSU} = \frac{((10000+DS_{NMRPPSU}\times 80)\times IEC-(DS_{NMRPPSU}\times m)\times 1000)}{((1000-80\times IEC)\times n)} \quad (5)$$

where 10000 is the backbone average molecular weight of the PSU and PPSU blocks, 80 g mol^{-1} is the molecular weight of the sulfonic group, m = 12.5 and n = 11.3 are the number of the structural units of PPSU and PSU blocks, respectively, and the averaged IEC value is used.

Table 2. IEC, DS_{PSU} and DS_{PPSU} values of SPES copolymers

Membrane	IEC[a] (meq. H^+ g^{-1})	IEC[b] (meq. H^+ g^{-1})	$IEC_{average}$ (meq. H^+ g^{-1})	DS_{PSU}	DS_{PPSU}
SPES 1	1.01	0.94	0.97	0.75	0.18
SPES 2	1.48	1.44	1.46	0.81	0.61
SPES 3	1.58	1.65	1.62	0.76	0.82

[a] Standard titration; [b] Titration in organic medium.

Based on these results, sulfonation occurs preferentially on the PSU blocks, and once the PSU DS exceeds 0.5, the reaction is no longer regioselective. Thus, it can be inferred that when trimethylsilylsulfonate is incorporated (every two structural units), its electron-withdrawing effect counterbalances the electron-donating inductive effect of isopropylidene in the PSU units. At that point, the PPSU repeat units begin to react with TMSCS. In addition, both blocks are susceptible to sulfonation due to the excess TMSCS used in the reaction. This might be ascribed to the TMSCS dielectric constant that results in an overall polarity increase, favouring and levelling sulfonation on both blocks [26]. These described issues lead to, in the case of the SPES 3 membrane, close DS on each block. Sulfonation is also confirmed by FTIR. Pristine PES is compared

with SPES ionomers specifically in the frequency range of 1040-1000 cm^{-1} in Figure 2S of the supporting information. Two bands are observed. PES exhibits a single band at 1014 cm^{-1}, associated with the symmetric stretching vibration of the diphenyl-ether units. This band is also observed in SPES, in addition to a band centred at 1028 cm^{-1}, which is ascribed to the symmetric stretching vibration of the sulfonic groups [41]. The intensity of this band increases with IEC from SPES 1 to 3.

3.1.2.2. Molecular Weight Distribution (MWD)

MWD and polydispersity index, I_p (M_w/M_n), determined by SEC and SEC-MALLS are gathered in Table 3. Cyclization and difficulties in perfectly balance monomer stoichiometry are well known challenges. For this reason, polycondensation leads to molecular weights that are significantly lower than polymers prepared by free-radical, anionic, or cationic initiation. Iojoiu et al [30] noted the decisive role of chain lengths on membrane durability. Thus, SPES based on PSU-3500 (DS=0.58) with a number average molecular weight (M_n) of 19900 and 38000 g mol^{-1} were compared. Classical SEC is first performed and molecular weights were calculated in equivalent polystyrene, as the Mark-Houwink-Sakurada (MHS) constants of our polycondensated multiblock copolymers are unknown. However, this routine analysis neglects changes in hydrodynamic volumes regarding, on the one hand, polymeric backbones PSU/PPSU blocks vs polystyrene and, on the other hand, non-ionic polymers and ionomers. SEC-MALLS does not require any calibration and should provide the actual MWD. With the pristine polycondensated multiblock (Table 3), SEC-MALLS provides higher molecular weights than SEC (~50%), in agreement with PSU-3500 data [30]. More surprising is the gap between I_p, as polydispersity index is almost independent of MHS constants. Light scattering (LS) is very sensitive to high molecular weight aggregates that increase both weight average molecular weight (M_w) and I_p. Indeed, comparing the LS curve and

refractive index curve (which measures the amount of polymer), a gap is observed, confirming the presence of aggregates that were previously ascribed to chains end-capped by phenol, leading to inter-chain hydrogen bonding. Even though the multiblock microstructures of our polymers make it difficult to accurately assessing their MWD, both techniques allowed the determination of M_n values (weakly impacted by aggregates). These M_n values are five-fold and fourfold higher than PSU-3500, as determined by SEC-MALLS and SEC, respectively. Following sulfonation, the molecular weights seemed to slightly decrease when they should increase. Even though it is impossible to discard possible chain breaks, it must be emphasized that great attention was paid to maintaining of a sufficient argon flux to remove the HCl by-product. Nonetheless, the SPES 1 sample seems to have undergone chain breaks during sulfonation. However, samples analysed in exhibit M_n values two- (SPES 1) to three-fold (SPES 2 and 3) higher than the best values obtained from PSU-3500. The absence of oligomers can be inferred from the unimodal SEC curves. This would be an indisputable asset, as sulfonic acid oligomers progressively eluted during PEMFC operation and are detrimental to the membrane homogeneity and lifetime.

Table 3. Number (M_n) and weight (M_w) average molecular weight of PSU/PPSU and SPSU/SPPSU copolymers. Polydispersity index (I_p) was also calculated

Polymer	M_n[a] $\times 10^3$(g mol^{-1})	M_n[b] $\times 10^3$(g mol^{-1})	M_w[a] $\times 10^3$(g mol^{-1})	M_w[b] $\times 10^3$(g mol^{-1})	I_p[a]	I_p[b]
PES	177	121	528	329	2.9	2.7
SPES 1	61	94	117	221	1.9	2.3
SPES 2	115	136	279	339	2.4	2.4
SPES 3	118	85	165	210	1.4	2.4

[a] Real; [b] Calculated in polystyrene equivalents.

3.2 Thermal properties

The thermal stability of the membranes is studied by thermogravimetric analysis, TGA. The TGA curves for PSU/PPSU and SPES 1, 2, and 3 membranes are given in Figure 3. The non-sulfonated copolymer shows the main weight loss between 400 and 500 ˚C, which corresponds to decomposition of the polymer backbone. Regarding the sulfonated membranes, three weight-loss steps are observed in these samples. The first weight loss, below 150 ˚C, is attributed to water elimination, and the second weight loss, between 200 and 400 ˚C, is assigned to the sulfonic group degradation, while the third loss, observed approximately 500 ˚C can be associated with decomposition of the polymer backbone. ~~However, the first weight loss, which appears near 300 ˚C, can be associated with degradation of the polymer chains into lower molecular weights [40].~~ The thermal decomposition of the sulfonic groups (T_{OD} and T_{FD} values are higher than 240 ˚C and 260 ˚C, respectively (Table 4)) are in accordance with published data on SPSU, PSU and fluorinated PES copolymers [27,20,21]. This behaviour is similar to that reported for other PEMs based on PES block copolymers. Thus, multiblock copoly(arylene ether sulfone)s show $T_{d5\%}$ values above 310 ˚C under similar experimental conditions [42]. In addition, TGA under isothermal conditions are performed at 100 ˚C, and after 12 h, a loss between 1.3-2.8% (Table 4) is observed, very close to the weight loss in the first step on the kinetic curve (Figure 3).

Table 4. Thermal parameters of SPES membranes

Membrane	T_{OD} (˚C)[a]	T_{FD} (˚C)[b]	$T_{d5\%}$ (˚C)	Weight loss %[b]	T_g (˚C)
SPES 1	245	333	300	1.35	184
SPES 2	241	288	291	2.79	185

SPES 3	240	262	333	2.12	187

[a] Sulfonic groups; [b] T = 100 ºC and t = 12 h.

The thermal transitions of the sulfonated copolymers are analysed by DSC. SPES membranes show only one glass transition temperature (T_g) ranging from 184 to 187 ˚C as a function of IEC values (Table 4). These values are close to that of PSU, i.e., 186 ˚C, as determined in the same conditions [43]. The presence of a single T_g tends to illustrate the absence of phase separation between the two blocks. However, the T_g of the two blocks are probably very close, leading to overlapping.

3.3 Membrane morphology

The morphology of the membranes has been examined via scanning electron microscopy. Aspects such as the homogeneity, the phase separation between hydrophobic and hydrophilic microstructures [44], or the presence of clusters [19], are essential to understanding the properties of the membranes, e.g., proton conductivity, mechanical properties and fuel cell performance. The FEG-SEM image of the SPES 2 membrane at the surface is shown in Figure 3S of the supporting information. Sulfonated copolymers show a tight, homogeneous structure with no apparent cracks and pores. In accordance with the obtained DS values, both blocks are sulfonated, and thus the phase separation between PSU and PPSU blocks is poor or non-existent. This result is in agreement with the presence of a unique T_g as determined by DSC analysis (Table 4).

3.4 WU%

The water absorption of a proton exchange membrane is crucial for proper operation in a fuel cell and clearly affects ionic conductivity, mechanical properties and fuel cell performance. The WU% values at two different temperatures are displayed in Table 5. At 30 ˚C, WU% increased from 5.50 to 23.90% as IEC increased from 0.97 to 1.62. This tendency is related to increase hydrophilicity (in acceptor number, AN), although increased polarity has also been evoked [45]. Thus, highly sulfonated membranes show higher hydrophilicity and, consequently, higher WU%. At 60 ˚C, no significant differences between SPES 1 and SPES 2 are observed (11.00 and 11.60%, respectively). However, hydration ability is favoured compared with 30 ˚C values (5.50 and 7.00%). Thus, at low DS (SPES 1 and 2), the influence of temperature does not show a clear tendency. This might be ascribed to the limited content in hydrophilic sulfonic acids and to the high molecular weight of the copolymers, hence the high entanglement level. Nevertheless, at high DS (SPES 3) the WU% is significantly higher than at low DS and it increases from 23.90% to 31.20% between 30 ˚C and 60 ˚C. This means that the effect of temperature is clearer when the number of sulfonated groups increases. Notably, the WU% of our copolymers is much lower than that reported for sulfonated commercial PSU [46]. Thus, sulfonated PSU, with similar IECs to those of SPES 1 and 2, showed WU% of 17.4 and 61.1%, respectively [47]. The much lower WU% of our copolymers can be ascribed to their multiblock microstructure (although both blocks are sulfonated) as well as their fairly high molecular weight [31].

3.5 Mechanical Properties

The thermo-mechanical characteristics of membranes are essential, as they govern their performances and durability in PEMFC. Thus, high TS (in a wide range of temperature, humidity), and ductility allow the shaping of ionomers into thin and non-

brittle films. This fact contributes to minimizing the ohmic drop in the electrolyte. Membranes must adapt to changes in relative humidity and temperature while maintaining their dimensional stability. To assess their mechanical performance, both stress-strain tests and dynamo mechanical tests have been conducted.

3.5.1 Stress-Strain Tests

The mechanical properties of a fuel cell membrane clearly depend on their ability to absorb water [4]. Thus, stress-strain tests are performed on the membranes in dry and wet forms (SPES-Na and SPES-H, respectively). Thus, tensile stress-strain curves for both dry and wet SPES 1 membranes are compared in Figure 4. In general, dry membranes exhibit higher tensile strength and higher stiffness (slope of the linear part of the stress-strain curve) than wet membranes. As a small molecule strongly interacting with the hydrophilic sulfonic groups, water should indeed plasticize SPES-H, even though it increases SO_3H dissociation. Narducci et al. ascribes the water plasticizing effect to a decrease in Van der Waals interactions between macromolecular chains, as induced by its high dielectric constant [48]. This tendency is observed for all sulfonated membranes (Table 5). The most pronounced effect is observed for SPES 3 (TS decreases by approximately 36% due to the higher WU%). The TS depends also on the IEC. Thus, TS increases from 66 to 87 MPa for dry membranes when the IEC increases from 0.97 to 1.62 meq H^+ g^{-1}. The increase in TS with IEC can be explained by considering the interactions of sulfonic groups in the polymer matrix [31,33]. These TS values can be compared with the value for Nafion 112 with a similar thickness, showing greater TS for SPES (Table 5). In the case of wet SPES-H membranes, tensile strengths are considerably higher than for other wet membranes based on similar polymeric backbones, for instance sulfonated polyphenylsulfone (TS of 13 MPa) [49],

SPSU (TS = 11 MPa) [27] or sulfonated PEEK-b-PES copolymers (TS values ranging from 23.8 to 35.4 MPa) [33].

SPES-Na membranes in the dry form have low ductility. Thus, elongations at break (ε) are lower than 5% for all samples (Table 5). However, wet membranes are much more ductile. Thus, ε for SPES-H 2 membrane is 57%, while the high ductility of SPES-H 3 impedes obtaining a reliable ε. Guo and coworkers [33] reported similar ε values for wet sulfonated PEEK-b-PES copolymers (ε ranging from 20.1 to 51.8%). However, these membranes are not sulfonated on the polymeric backbones but rather on the anisole groups.

Table 5. WU% values and mechanical properties of dry and wet SPES membranes; Tensile Strength (TS) and Elongation at Break (ε), Storage Modulus at 50 ˚C ($E'_{50^\circ C}$) and Temperature associated with a α Relaxation (T_α) (from DMTA Experiments)

Membrane	WU %		TS[a] (MPa)		ε[a] %		$E'_{50^\circ C}$ (MPa)		$T_{\alpha\ \mathrm{DMTA}}$ (˚C)	
	30˚C	60˚C	Dry Na^+	Wet H^+	Dry Na^+	Wet H^+	Dry Na^+	Wet H^+	Dry Na^+	Wet H^+
SPES 1	5.50	11.00	66	55	5.0	15.0	2986	2427	205	219
SPES 2	7.00	11.60	74	67	3.5	57.0	3210	2414	226	221
SPES 3	23.90	31.20	87	56	3.7	-	5004	3424	230	223
Nafion 112[b]	-	-	19	-	-	-	-	-	-	-

[a] T = 30 ˚C; [b] TS determined in H^+ form [50]

3.5.2 Dynamic Mechanical Analysis

To evaluate the thermo-mechanical properties and relaxation processes of sodium and proton forms of SPES membranes (SPES-Na and SPES-H, respectively), the variation of storage (E'), and loss modulus (E'') with temperature is studied. Indeed, the Na^+ form undergoes much easier drying. As an example, Figure 5 displays DMA curves for SPES-Na and SPES-H 1. The drop in storage modulus and peak of loss modulus are directly related to the α relaxation process associated with the T_g of SPES-Na and SPES-H, respectively. For each membrane, T_g is determined from the peak of the loss modulus and reported in Table 5, as is the storage modulus.

The storage modulus at 50 ˚C ($E'_{50°C}$) appears to depend on the presence of sodium sulfonate groups, which increase with IEC. Thus, α relaxation temperatures of SPES-Na (T_α), associated with T_g are gathered in Table 5. T_α increases from 205 to 230 ˚C with the content in sodium sulfonate groups, i.e., from SPES 1 to 3. Once characterized in the sodium forms, the acidic ionomers (SPES-H) are also tested. It is well-known that in ionomers based on homopolymer (due to the increase in ionicity), T_g increases substantially from acidic forms to salts. Thus, in the series of acrylate and methacrylate, T_g shifts from 105 to 230 ˚C and from 228 to 310 ˚C, respectively, when moving from the acidic form to sodium one [51]. However, the increase in ionicity is mitigated by the stiffness of the backbone, as highlighted by the gap decrease in polymethacrylate compared to acrylate and as previously observed in the H^+ and Na^+ form for SPSU [26]. Indeed, in the case of SPES-H, from DMA curves, a very slight decrease in E' is observed between room temperature and approximately 200 ˚C with respect to the SPES-Na form. Surprisingly, creeping is delayed from approximately 20 ˚C in the case of SPES-H. This can be ascribed to inter-chain hydrogen bonding, and possibly to partial crosslinking induced by the formation of anhydrides at high temperature [52]. Nonetheless, the membranes in their dry state exhibit sufficient

strength to be operated in FCs, especially as WU% is much more limited than in SPSU based on PSU homopolymer [27].

3.6 Proton conductivity of SPES membranes

The proton conductivity of the SPES membranes is determined by EIS. The evolution of ionic conductivity with temperature (Figure 6A) and relative humidity (Figure 6B) for the three different membranes is displayed in Figure 6. EIS measurements are performed using a homemade device whose accuracy was previously established [53]. As shown in the Arrhenius plots in Figure 6A, conductivity increases, as expected, with IEC; the gap is more pronounced between the SPES 1 and SPES 2. Indeed, sulfonation of both blocks (DS > 0.5) and resulting higher WU% lead to better percolation of ionic domains and a lower tortuosity. The maximum ionic conductivity is at 95% RH and 80 ˚C, namely 25 mS cm^{-1} for SPES 3 (Table 6). However, these values are higher than those reported for SPSU [30]. Moreover, these membranes, even in a hydrated state, exhibit very good mechanical strength (Table 5) and no brittleness.

The conductivity dependence on RH is also evaluated (Figure 6B), and the conductivity increased markedly from 30 to 95% RH. In the case of the SPES 3 membrane, the conductivity increases by an order magnitude.

3.7 Fuel Cell test

The SPES 3 membrane, combining high conductivity and excellent mechanical properties, is selected for the fuel cell. For comparison with our membrane, measurements of Nafion 112 and 117 are performed in the same conditions. MEA based on a 5 cm^2 active area single cell is evaluated at temperatures from 50 to 80 ˚C, under

100% RH and at atmospheric pressure. Figure 7 shows voltage-current density (A) and power density-current density (B) curves. As shown in this figure, fuel cell performance improves with temperature up to 70 ˚C, where the maximum power density (~ 400 mW cm^{-2}) and the maximum current density (1100 mA cm^{-2}) are achieved.

These results are much better than those reported on sulfonated cardo PEEK-WC-PES random copolymers, which showed a maximum power density of 90 mW cm^{-2} and a maximum current density of 340 mA cm^{-2} at 50 ˚C and 100% RH [36]. Notably, the results are very promising, especially compared to commercial membranes with similar thickness such as Nafion 112 (power density of 729 mW cm^{-2} and a current density of 2400 mA cm^{-2} at 70 ˚C and 100% RH) and the thicker Nafion 117 (power density of 310 mW cm^{-2} and a current density of approximately 999 mA cm^{-2} at 70 ˚C and 100% RH), which are often used as reference materials. From these comparative MEA tests, it can be concluded that a membrane based on SPES copolymers exhibit satisfying performance.

In situ through-plane proton conductivity of SPES 3 membrane ($\sigma_{m\ MEA}$) is determined on the MEA by EIS using the same cell hardware as fuel cell tests and H_2/N_2 gases. Table 6 compares the ionic conductivity values of SPES 3 membrane obtained by both ex situ and in situ measurements at different temperatures, at atmospheric pressure and under humidified gases (100% RH). In addition, the in situ proton conductivities of Nafion 112 and 117 are included in Table 6 as reference materials. The hydration of our membrane at 50 ˚C is higher than in Nafion 117. Thus, the temperature required to register a value of conductivity for SPES membranes is lower. The aforementioned experimental conditions allowed us to obtain approximate conductivities in conditions close to MEA operation (see section 3.5) (Table 6). As shown in this table, close ionic conductivities are obtained using blocking electrodes

and an MEA cell. The $\sigma_{m\ MEA}$ increases considerably when the temperature varied from 50 to 80 ˚C. Nevertheless, at temperatures above 70 ˚C, conductivity does not improve. At 70 ˚C and 100% RH, the SPES 3 membrane achieves a value of 34.1 mS cm^{-1} for $\sigma_{m\ MEA}$. This value is slightly lower than that measured under the same conditions for Nafion 117 (σ_{MEA}= 57.3 mS cm^{-1}) and similar to that observed for Nafion 112 (σ_{MEA}= 34.0 mS cm^{-1}), which are considered a reference material. Thus, these new copolymers show satisfactory conductivity and electrochemical performance for use as conducting membranes in fuel cells.

Table 6. Proton conductivity of SPES 3 membrane obtained by ex situ (σ_m) and in situ ($\sigma_{m\ MEA}$) measurements

T (˚C)	σ_m [a] (mS cm^{-1})	$10^2 \times$ R (Ω)	$\sigma_{m\ MEA}$ [b] (mS cm^{-1})	σ^{N112}_{MEA} (mS cm^{-1})	σ^{N117}_{MEA} (mS cm^{-1})
50	19.2	6.00	19.7	-	-
60	23.4	4.58	25.8	33.0	55.3
70	24.5	3.47	34.1	34.0	57.3
80	25.4	3.97	29.8	34.3	52.6

[a] Determined as described in section 3.5. [b] 59.2 μm of thickness

4. Conclusions

This study targeted ionomers based on multiblock polycondensates that could be produced at industrial scale. Indeed, the one-pot two-step synthesis allows (i) using available monomers and (ii) avoiding the use of ionic monomers. In fact, obtaining high molecular weight polycondensates requires the best stoichiometric balance possible and, therefore highly pure monomers, while scaling up ionic monomer purification is often difficult and costly. For that purpose, the commercial, cheap, and very pure monomers

used in Udel® and Radel® production are reacted using a "one-pot two-step synthesis" approach. This led to high molecular weight multiblock polyethersulfone that is further sulfonated. Using mild sulfonation conditions (moderate reaction temperature, mild sulfonating reactant, low concentration of TMSCS) we bet on the lesser reactivity of the PPSU repeat unit towards electrophilic substitution compared to PSU. Therefore, no microphase separation is detected on the most conductive ionomer. Although separation does not occur, the resulting ionomers exhibit good performances in terms of WU% and mechanical strength. SPES shows a tensile strength of 56 MPa, considerably higher than those observed for SPSU, which showed a TS of 11 MPa and sulfonated PEEK-b-PES copolymers whose TS ranges between 23.8 and 35.4 MPa. The preliminary MEA tests perform on the highest sulfonated ionomer are promising, as power and current density of 400 mW cm^{-2} and 1100 mA cm^{-2}, respectively, are achieved at 70 ˚C. While many experiments have already been performed, the material can be further refined. Thus, we are currently testing some strategies (e.g., still milder sulfonation conditions to favour PSU sulfonation) to generate better immiscibility between blocks to induce an actual microphase separation.

Acknowledgements

This work was supported by mobility grant of IAAB from Universidad Carlos III de Madrid and the Projects from the regional government [Comunidad de Madrid through MATERYENER3CM S2013/MIT-2753 and S2013/MAE-2975 PILCONAER along with European Social Fund (ESF)]. In addition, funds from the Spanish Government, MINECO [MAT2016-78362-C4-3R and ENE2017-86711-C3-1-R] are gratefully acknowledged.

References

[1] IEA, CO_2 emissions from fuel combustion. Highlights. https://www.iea.org/, (accessed May 2018).

[2] M. Z. Jacobson, W.G. Colella, D. M. Golden, Cleaning the air and improving health with hydrogen fuel cell vehicles, Science 308 (2005) 1901-1905.

[3] M. A. Hickner, H. Ghassemi, Y. S. Kim, B. R. Einsla, J. E. McGrath, Alternative polymer systems for proton exchange membranes (PEMs), Chem. Rev. 104 (2004) 4587-4612.

[4] S. J. Peighambardoust, S. Rowshanzamir, M. Amjadi, Review of the proton exchange membranes for fuel cell applications, Int. J. Hydro. Energy 35 (2010) 9349-9384.

[5] S. Motupally, A. J. Becker, J. W. Beidner, Diffusion of water in Nafion-115 membranes, J. Electrochem. Soc. 147 (2000) 3171-3177.

[6] P. Choi, N. H. Jalani, R. Datta, Thermodynamics and proton transport in Nafion II. Proton diffusion mechanisms and conductivity, J. Electrochem. Soc. 152 (2005) 123-130.

[7] J. Wu, X. Z. Yuan, J. J. Martin, H. Wang, J. Zhang, J. Shen, S. Wu, W. Merida, A review of PEM fuel cell durability: Degradation mechanisms and mitigation strategies, J. Power Sources 184 (2008) 104-119.

[8] E. Guilminot, A. Corcella, M. Chatenet, F. Maillard, F. Charlot, G. Berthomé, C. Iojoiu, J. Y. Sanchez, E. Rossinot, E. Claude, Membrane and active layer degradation upon PEMFC steady-state operation, J. Electrochem. Soc. 154 (2007) 1106-1114.

[9] E. Guilminot, A. Corcella, F. Charlot, F. Maillard, M. Chatenet, Detection of

Pt^{z+} ions and Pt nanoparticles inside the membrane of a used PEMFC, J. Electrochem. Soc. 154 (2007) 96-105.

[10] A. Kraytsberg, Y. E. Eli, Review of Advanced Materials for Proton Exchange Membrane Fuel Cells, Energy Fuels 28 (2014) 7303-7330.

[11] C. Iojoiu, Modern synthesis processes and reactivity of fluorinated compounds, H. Groult, F. Leroux and A. Tressaud (Eds), El servier, 1st edition, France, 2016, 16, 465-497.

[12] G. A. Giffin, S. Galbiati, M. Walter. K. Aniol, C. Ellwein, J. Kerres, R. Zeis, Interplay between structure and properties in acid-base blend PBI-based membranes for HT-PEM fuel cells, J. Membr. Sci. 535 (2017) 122-131.

[13] J. P. Melchior, G. Majer, K. D. Kreuer, Why do proton conducting polybenzimidazole phosphoric acid membranes perform well in high-temperature PEM fuel cells?, Phys. Chem. Chem. Phys. 19 (2016) 601-612.

[14] P. X. Xing, G. P, Robertson, M. D. Guiver, S. D. Mikhailenko, K. P. Wang, S. Kaliaguine, Synthesis and characterization of sulfonated poly(ether ether ketone) for proton exchange membranes, J. Membr. Sci. 229 (2004) 95-106.

[15] R. C. Jiang, H. R. Kunz, J. M. Fenton, Investigation of membrane property and fuel cell behavior with sulfonated poly(ether ether ketone) electrolyte: Temperature and relative humidity effects, J. Power Sources 150 (2005) 120-128.

[16] H. L. Wu, C. C. M. Ma, F. Y. Liu, C. Y. Chen, S. J. Lee, C. L. Chiang, Preparation and characterization of poly(ether sulfone)/sulfonated poly(ether ether ketone) blend membranes, Eur. Polym. J. 42 (2006) 1688-1695.

[17] Y. Li, Q. T. Nguyen, P. Schaetzel, C. Lixon-Buquet, L. Colasse, V. Ratieuville, S. Marais, Proton exchange membranes from sulfonated polyetheretherketone and sulfonated polyethersulfone-cardo blends: Conductivity, water sorption and permeation properties, Electrochim. Acta 111 (2013) 419-433.

[18] A. R. Kim, M. Vinothkannan, D. J. Yoo, Sulfonated-fluorinated copolymer blending membranes containing SPEEK for use as the electrolyte in polymer electrolyte fuel cells (PEFC), Int. J. Hydro. Energy 42 (2017) 4349-4365.

[19] J. J. R. Arias, J. C. Dutra, A. D. S. Gomes, Hybrid membranes of sulfonated poly ether ether ketone, ionic liquid and organically modified montmorillonite for proton exchange membranes with enhanced ionic conductivity and ionic liquid lixiviation protection, J. Membr. Sci. 537 (2017) 353-361.

[20] N. N. Krishnan, H. J. Kim, M. Prasanna, E. Cho, E. M. Shin, S. Y. Lee, I. H. Oh, S. A. Hong, T. H. Lim, Synthesis and characterization of sulfonated poly(ether sulfone) copolymer membranes for fuel cell applications, J. Power Sources 158 (2006) 1246-1250.

[21] N. N. Krishnan, H. J. Kim, J. H. Jang, S. Y. Lee, E. Cho, I. H. Oh, S. A. Hong, T. H. Lim, Sulfonated Poly(ether sulfone)-Based Catalyst Binder for a Proton-Exchange Membrane Fuel Cell, J. Appl. Polym. Sci. 113 (2009) 2499-2506.

[22] B. Baradie, C. Poinsignon, J. Y. Sánchez, Y. Piffard, G. Vitter, N. Bestaoui, D. Foscallo, A. Denoyelle, D. Delabouglise, M. Vaujany, Thermostable ionomeric filled membrane for H_2/O_2 fuel cell, J. Power Sources 74 (1998) 8-16.

[23] P. Genova-Dimitrova, B. Baradie, D. Foscallo, C. Poinsignon, J. Y. Sanchez, Ionomeric membranes for proton exchange membrane fuel cell (PEMFC): sulfonated polysulfone associated with phosphatoantimonic acid, J. Membr. Sci. 185 (2001) 59-71.

[24] F. Lufrano, I. Gatto, P. Staiti, V. Antonucci, E. Passalacqua, Sulfonated polysulfone ionomer membranes for fuel cells, Solid State Ionics 145 (2001) 47-51.

[25] B. Smitha, S. Sridhar, A. A. Khan, Synthesis and characterization of proton conducting polymer membranes for fuel cells, J. Membr. Sci. 225 (2003) 63-76.

[26] C. Iojoiu, M. Maréchal, F. Chabert, J. Y. Sanchez, Mastering sulfonation of aromatic polysulfones: Crucial for membranes for fuel cell application, Fuel cells 5 (2005) 344-354.

[27] A. M. Martos, J. Y. Sanchez, A. Várez, B. Levenfeld, Electrochemical and structural characterization of sulfonated polysulfone, Polym. Testing 45 (2015) 185-193.

[28] X. Li, C. Zhao, H. Lu, Z. Wang, H. Na, Direct synthesis of sulfonated poly(ether ether ketone ketone)s (SPEEKKs) proton exchange membranes for fuel cell application, Polymer 46 (2005) 5820-5827.

[29] W. L. Harrison, F. Wang, J. B. Mecham, V. A. Bhanu, M. Hill, Y. S. Kim, J. E. McGrath, Influence of the bisphenol structure on the direct synthesis of sulfonated poly(arylene ether) copolymers, J. Polym. Sci. A Polym. Chem. 41 (2003) 2264-2276.

[30] C. Iojoiu, P. Genova-Dimitrova, M. Maréchal, J. Y. Sánchez, Chemical and physicochemical characterizations of ionomers, Electrochim. Acta 5 (2006) 4789-4801.

[31] L. Assumma, C. Iojoiu, R. Mercier, S. Lyonnard, H. D. Nguyen, E. Planes, Synthesis of partially fluorinated poly(arylene ether sulfone) multiblock copolymers bearing perfluorosulfonic functions, J. Polym. Sci. Part A: Polym. Chem. 53 (2015) 1941-1956.

[32] A. Sannigrahi, S. Takamuku, P. Jannasch, Block copolymers combining semi-fluorinated poly(arylene ether) and sulfonated poly(arylene ether sulfone) segments for proton exchange membranes, Int. J. Hydro. Energy 39 (2014) 15718-15727.

[33] M. Guo, X. Li, L. Li, Y. Yu, Y. Song, B. Liu, Z. Jiang, Novel postsulfonated poly(ether ether ketone)-block-poly(ether sulfone)s as proton exchange membranes for fuel cells: Design, preparation and properties, J. Membr. Sci. 380 (2011) 171-180.

[34] S. Y. Chao, D. R. Elsey, Process for preparing sulfonated poly(arylether) resins, United States patent US 4,625, 000, 1996 Nov 25.

[35] F. J. Fernández, V. Compan, E. Riande, Hybrid ion-exchange membranes for fuel cell and separation processes, J. Power Scources 173 (2007) 68-76.

[36] A. M. Martos, M. Biasizzo, F. Trotta, C. del Río, A. Várez, B. Levenfeld, Synthesis and characterization of sulfonated PEEK-WC-PES copolymers for fuel cell proton exchange membrane application, Eur. Polym. J. 93 (2017) 390-402.

[37] K. Prashantha, S. G. Park, Nanosized TiO_2-filled sulfonated polyethersulfone proton conducting for direct methanol fuel cells, J. Appl Polym. Sci. 98 (2005) 1875-1878.

[38] N. Cornet, G. Beaudoing, G. Gebel, Influence of the structure of sulfonated polyimide membranes on transport properties, Sep. Purif. Technol. 22-23 (2001) 681-687.

[39] A. Jasti, S. Prakash, V. K. Shahi, Stable and hydroxide ion conductive membranes for fuel cell applications: Chloromethylation and amination of poly(ether ether ketone), J. Memb. Sci. 428 (2013) 470-479.

[40] A. Noshay, L. M. Robeson, Sulfonated polysulfone, J. Appl. Polym. Sci. 20 (1976) 1885-1903.

[41] Y. Devrim, S. Erkan, N. Bac, I. Eroglu, Preparation and characterization of sulfonated polysulfone titanium dioxide composite membranes for proton exchange membrane fuel cells, Int. J. Hydrogen Energy 34 (2009) 3467-3475.

~~[40] M. Maréchal, R. Wessel, J. P. Diard, J. Guindet, J. Y. Sanchez, Study of PEMFC ionomers through model molecules mimicking the ionomer repeat units, Electrochem. Acta 52 (2007) 7953-7963.~~

[42] S. Takamuku, P. Jannasch, Multiblock Copolymers with Highly Sulfonated Blocks Containing Di- and Tetrasulfonated Arylene Sulfone Segments for Proton Exchange Membrane Fuel Cell Applications, Adv. Energy Mater. 2 (2012) 129-140.

[43] M. T. Pérez-Prior, N. Ureña, M. Tannenberg, C del Río, B. Levenfeld, DABCO-functionalized polysulfones as anion-exchange membranes for fuel cell applications: Effect of crosslinking, J. Polym. Sci. Part B: Polym. Phys. 55 (2017) 1326-1336.

[44] K. D. Kreuer, On the development of proton conducting polymer membranes for hydrogen and methanol fuel cells, J. Membr. Sci. 185 (2001) 29-39.

[45] J. C. Tsai, J. F. Kuo, C. Y. Chen, Synthesis and properties of novel HMS-based sulfonated membranes poly (arylene ether sulfone)/silica nano-composite membranes for DMFC applications, J. Power Sources 174 (2007) 103-113.

[46] M. Herrero, A. M. Martos, A. Várez, J. C. Galván, B. Levenfeld, Synthesis and characterization of polysulfone/layered double hydroxides nanocomposite membranes for fuel cell application, Int. J. Hydrogen Energy 39 (2014) 4016-4022.

[47] A. M. Martos, Academic thesis: Synthesis and characterization of hybrid protonic membranes for fuel cell proton exchange membrane application, (https://e-archivo.uc3m.es/handle/10016/22531).Universidad de Carlos III de Madrid, 2015.

[48] R. Narducci, J. F. Chailan, A. Fahs, L. Pasquini, M. L. Di Vona, P. Knauth, Mechanical properties of anion exchange membranes by combination of tensile stress-strain tests and dynamic mechanical analysis, J. Polym. Sci. Part B: Polym. Phys. 54 (2016) 1180-1187.

[49] M. L. Di Vona, E. Sgreccia, M. Tamilvanan, M. Khadhraoui, C. Chassigneux, P. Knauth, High ionic exchange capacity polyphenylsulfone (SPPSU) and polyethersulfone (SPES) cross-linked by annealing treatment: Thermal stability, hydration level and mechanical properties, J. Membr. Sci. 354 (2010) 134-141.

[50] D. J. Kim, H. J. Lee, S. Y. Nam, Sulfonated poly(arylene ether sulfone) membranes blended with hydrophobic polymers for direct methanol fuel cell applications, Int. J. Hydrogen Energy (2014) 17524-17532.

[51] Sigma Aldrich, https://www.sigmaaldrich.com/technical-documents/articles/materials-science/polymer-science/thermal-transitions-of-homopolymers.html, (accesed May 2018).

[52] F. M. Collete, C. Lorentz, G. Gebel, and F. Thominette, Hygrothermal aging of Nafion®, J. Membr. Sci. (2009) 21-29.

[53] M. Maréchal, J. L. Souquet, J. Guindet, J. Y. Sánchez, Solvation of sulphonic acid groups in Nafion® membranes from accurate conductivity measurements, Electrochem. Commun. 9 (2007) 1023-1028.

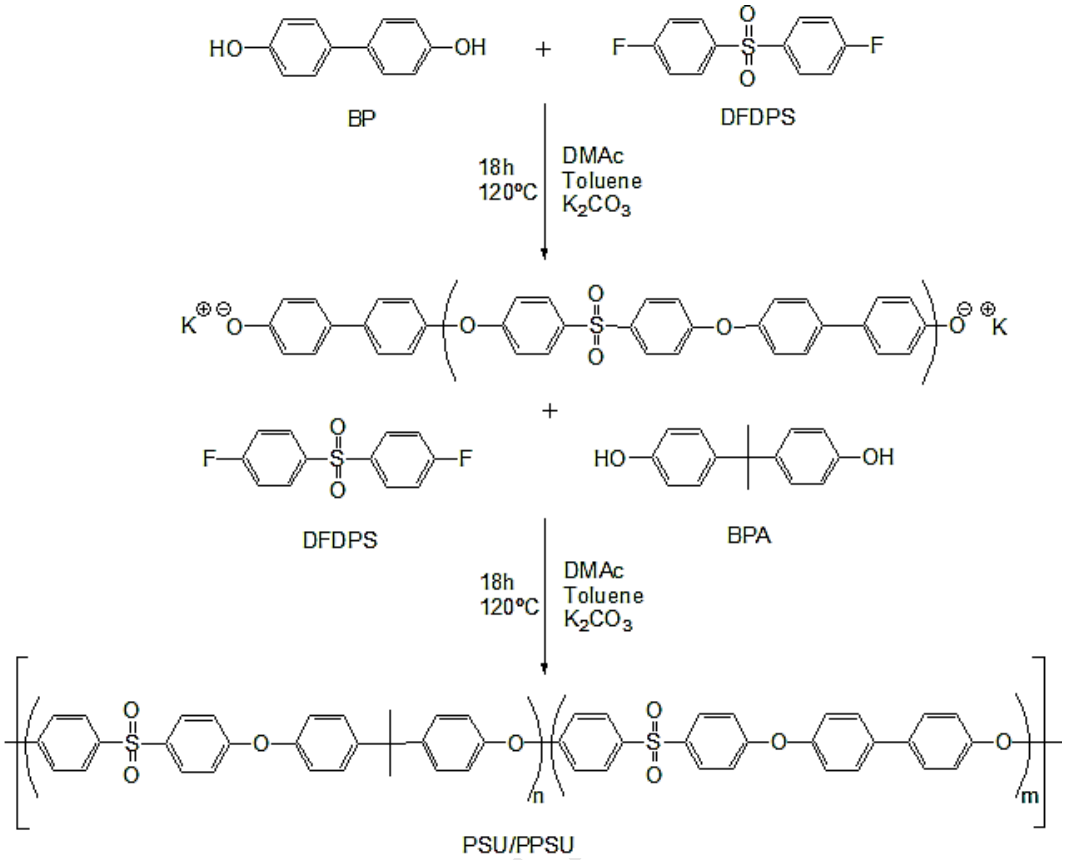

Scheme 1. Synthesis of PSU/PPSU.

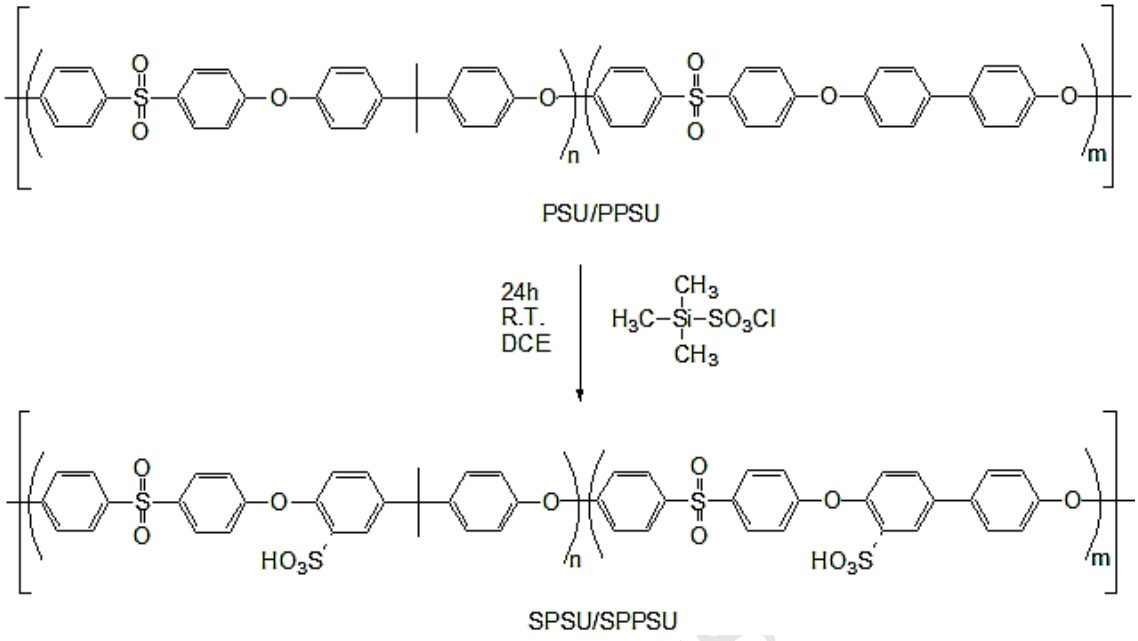

Scheme 2. Sulfonation of PSU/PPSU.

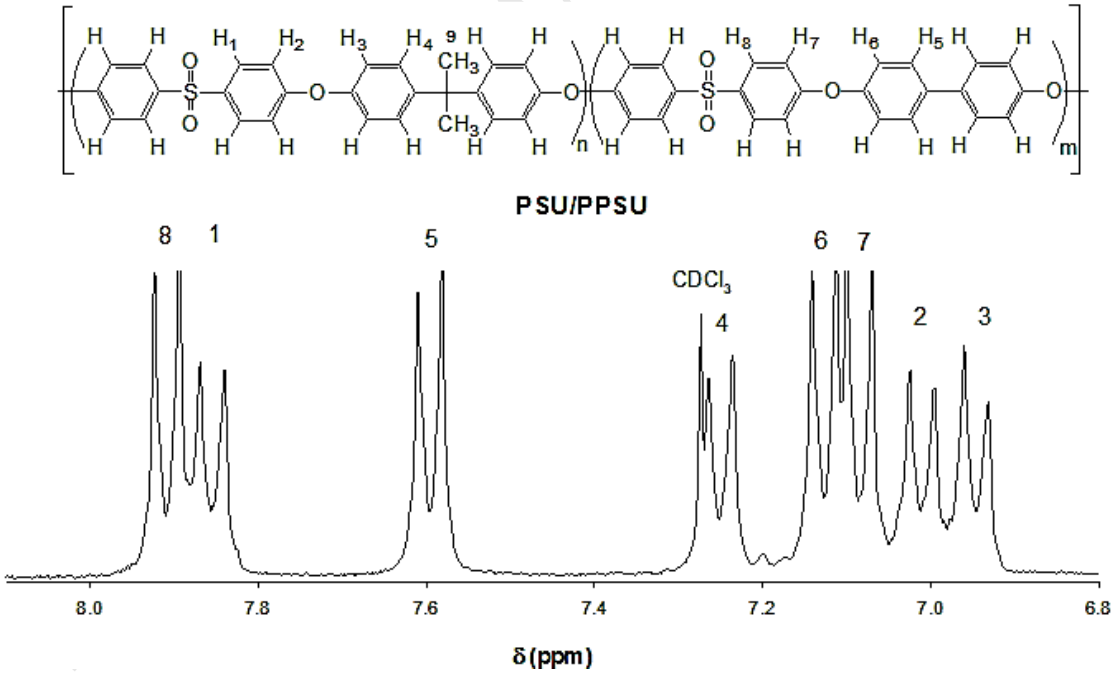

Figure 1. ^{1}H-NMR spectrum of PSU/PPSU (Solvent: $CDCl_3$).

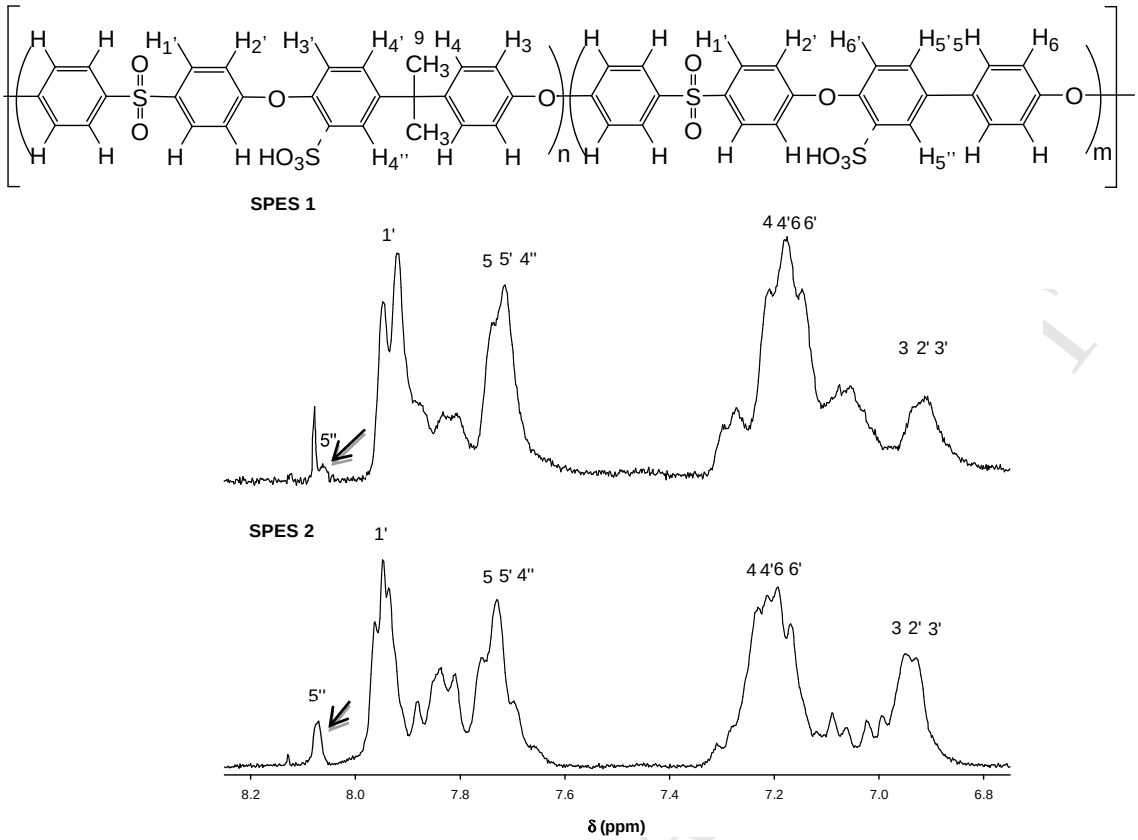

Figure 2. ^{1}H-NMR spectra of SPES 1, and 2 (Solvent: DMSO-d_6).

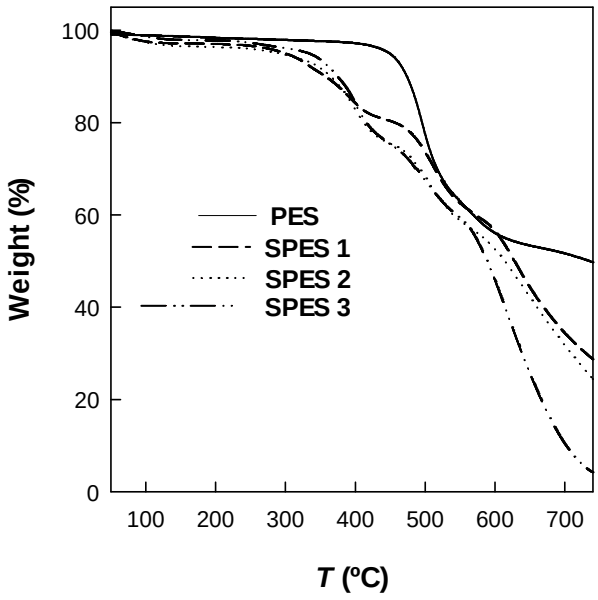

Figure 3. TGA curves for PSU/PPSU and SPES membranes under an air atmosphere.

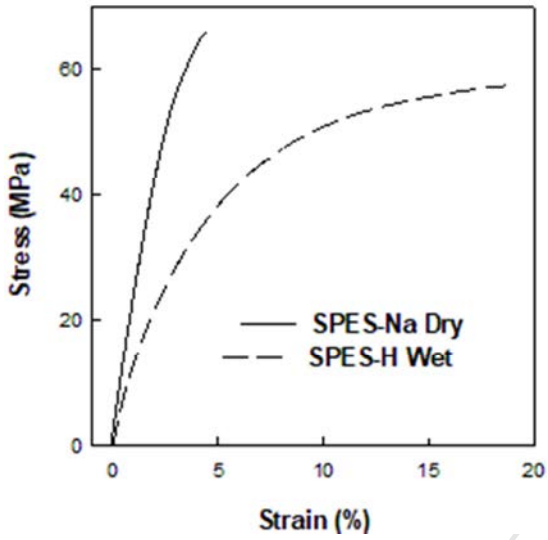

Figure 4. Tensile stress-strain curves for SPES 1 membranes at 30 ˚C.

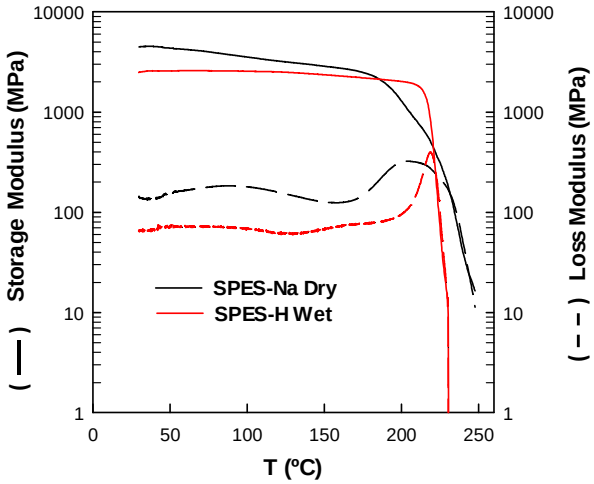

Figure 5. DMA curves for SPES 1 membrane.

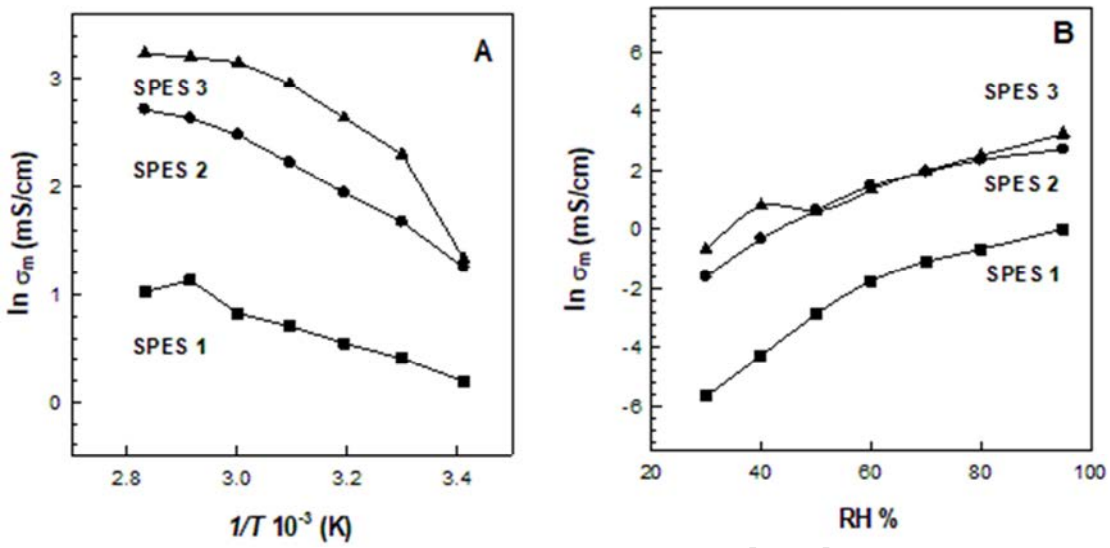

Figure 6. Proton conductivity of SPES 1 (■), 2 (●) and 3 (▲) membranes as a function of A) temperature at 95% RH and B) RH% at 80 ˚C.

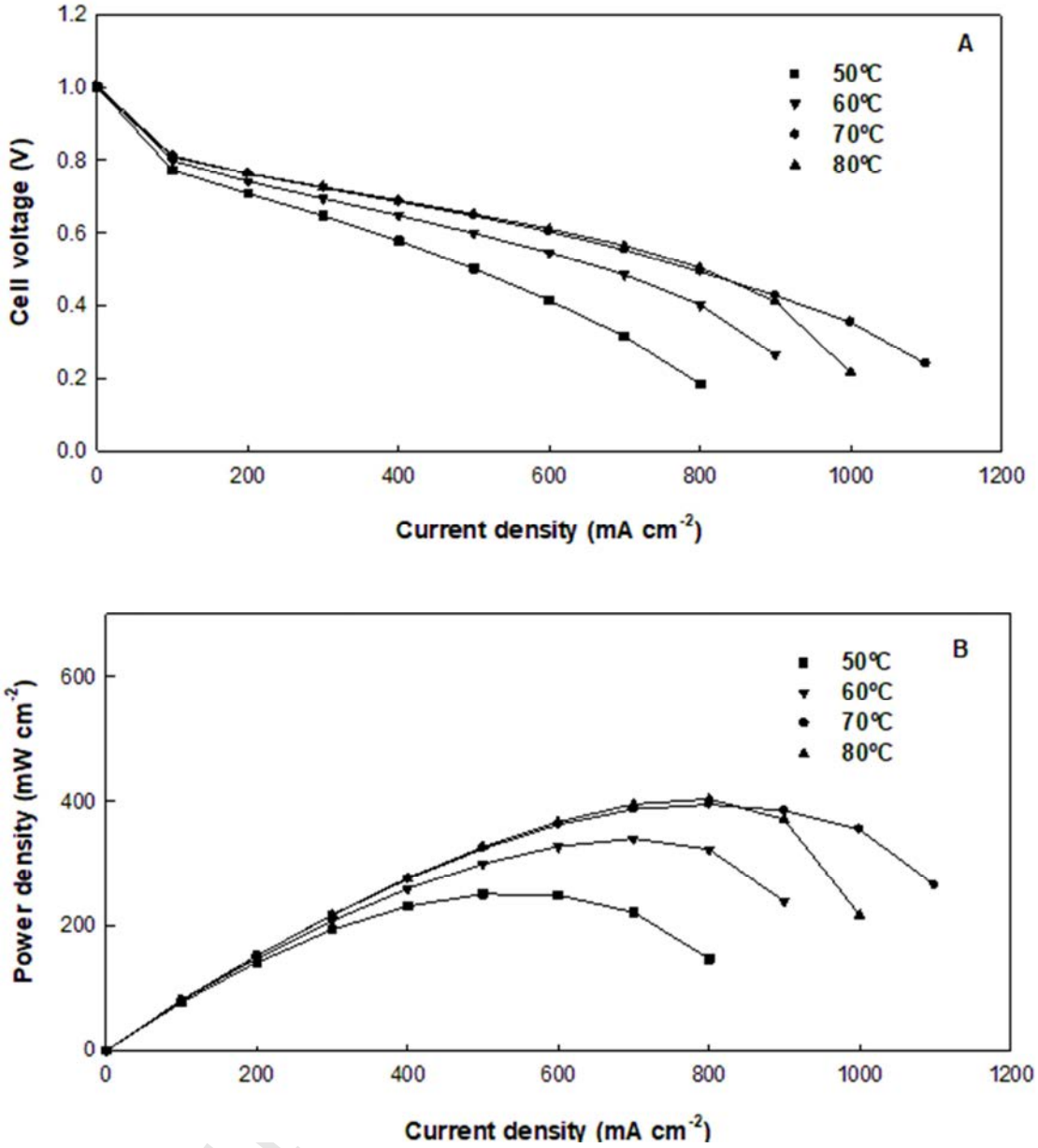

Figure 7. A) Polarization and B) power density curves of SPES 3 membrane at 50, 60, 70, and 80 ˚C and 100% RH.